CHAPTER

Retinal image preprocessing, enhancement, and registration 4

Carlos Hernandez-Matas[a], Antonis A. Argyros[a,b], Xenophon Zabulis[a]

[a]*Institute of Computer Science, Foundation for Research and Technology—Hellas (FORTH), Heraklion, Greece*

[b]*Computer Science Department, University of Crete, Heraklion, Greece*

1 Introduction

The first fundus images were acquired after the invention of the ophthalmoscope. The concept of storing and analyzing retinal images for diagnostic purposes exists ever since. The first work on retinal image processing was based on analog images and regarded the detection of vessels in fundus images with fluorescein [1]. The fluorescent agent enhances the appearance of vessels in the image, facilitating their detection and measurement by the medical professional or the computer. However, fluorescein angiography is an invasive and time-consuming procedure and is associated with the cost of the fluorescent agent and its administration.

Digital imaging and digital image processing have proliferated the use of retinal image analysis in screening and diagnosis. The ability to accurately analyze fundus images has promoted the use of noninvasive, fundus imaging in these domains. Moreover, the invention of new imaging modalities, such as optical coherence tomography (OCT) and scanning laser ophthalmoscopy (SLO), has broadened the scope and applications of retinal image processing. This review regards both fundus imaging, as implemented by fundus photography and SLO and OCT imaging.

Retinal image analysis supports pertinent diagnostic procedures. A number of symptoms and diseases are diagnosed through observation of the human retina. Retinal image analysis is useful not only in the diagnosis of ophthalmic diseases, but also in that of systemic chronic diseases. Hypertension and diabetes are two important examples of such diseases that affect small vessels and microcirculation and which are noninvasively screened and assessed through the contribution of retinal image analysis [2, 3]. In this context, two widely employed tasks are the detection and measurement of anatomical features and properties, such as lesion detection and measurement of vessel diameters. Achieving these tasks typically includes a preprocessing stage, tuned according to the measured features and the method of image analysis. This preprocessing stage usually regards the normalization of image

Computational Retinal Image Analysis. https://doi.org/10.1016/B978-0-08-102816-2.00004-6

intensities after image formation, as well as the enhancement of the image through noise reduction and contrast enhancement.

Image analysis methods capable of matching and aligning retinal images of the same eye have enabled the task of retinal image registration (RIR), which also plays a significant role in the diagnosis and the monitoring of diseases. By registering images acquired during the same examination, higher resolution and definition images of the retina can be obtained and enable high-precision measurements. Moreover, the registering images into mosaics facilitates mapping wider retinal regions than a single image does. Registration of images from different examinations facilitates follow-up examinations and assessment of treatment through the speed of symptom reversal.

2 Intensity normalization

Intensity normalization is the form of preprocessing closest to image acquisition, as it deals with the interpretation of pixel values for image formation. Digital sensors have built-in intensity normalization algorithms that subsequent image processing methods account for. Intensity normalization is also employed in the compensation of artifacts, due to uneven illumination of retinal tissue by the imaging modality.

2.1 Fundus imaging

The interplay between optics, light source, and eye shape casts illumination of the retina to be spatially uneven. This complicates feature detection and segmentation, often requiring local adaptation of processing.

Contrast normalization is usually applied to the "green" channel [4–7], as it is less sensitive to noise. Contrast enhancement in all three channels was proposed through 3D histogram equalization [8], or independent normalization of each channel [9]. In Ref. [10], intensity is adjusted based on information from the histograms of both red and green channels, in an attempt to reap benefits from information in both channels.

Generic, global approaches to intensity normalization have not fully solved this problem. Zero-mean normalization and unit variance normalization compensate only partially for lighting variation, as they introduce artifacts due to noise amplification [11–13]. A polynomial remapping of intensities [7] exhibits similar issues.

Generic, local approaches, based on the statistics of image neighborhoods, have been more effective and more widely adopted. To this end, Zhao et al. [14] employ a color-constancy method. Locally adaptive histogram equalization (CLAHE) [15] is one of the most widely used contrast normalization steps [16–23] including also adaptations of the initial method [24–26].

Retinal imaging-specific approaches estimate a model of illumination and rectify intensities according to the luminance it predicts [27–30]. This model is a mask image, where pixel values are estimates of tissue reflectivity. As the illumination source is usually unknown, this estimate is obtained assuming that local illumination variation is smaller than across the entire image.

2.2 Tomographic imaging

In OCT imaging, the need for intensity rectification stems from the automatic intensity rescaling and averaging of the sensor, which may differ in each scan. Generic intensity normalization has been applied to individual scans [31]. However, prominent noise reduction methods utilize multiple scans that image the same area and average measurements corresponding to the same tissue points [32–34]. The central step in such approaches is the registration of scans (see Section 4.2).

3 Noise reduction and contrast enhancement

Noise reduction and contrast enhancement are typical preprocessing steps in multiple domains of image analysis. Their goal is to improve image definition and fidelity, by accenting image structure and reducing image noise. Generic approaches to these tasks have been employed for all retinal image types. Nonetheless, approaches targeted to the particular modality and the subsequent analysis have been more widely adopted. Notably, in OCT imaging, noise reduction methods address an imaging artifact pertinent only to this modality, besides conventional image noise.

3.1 Fundus imaging

Generic approaches to local contrast and structural adjustment have been proposed [6, 7, 35–37], but are culpable in amplifying noise or noninteresting structures. Single-scale [38] and multi-scale [13, 39–41] linear filterings have also been tools of similar approaches but conversely they filter out useful fine image structure at fine scales. Morphological transformations have also been proposed, such as the contourlet [42] and the top-hat transformations [43], and were combined with histogram equalization [44] and matched filters [45]. Nonlinear filtering approaches have also been proposed. A diffusion-based “shock” filter was employed in Ref. [46]. In Ref. [47], inverse diffusion provided feature-preserving noise reduction. In Ref. [48], sparse coding and a representation dictionary were utilized to represent vessels and reconstruct the original image without noise.

Target-oriented contrast enhancement methods have also been tailored. Image sharpness was amplified by compensating for the blur of the eye’s point spread function, through the modeling of the former [49]. Multi-orientation filtering kernels that mimic and highly correlate with vessel intensity profiles were used in Refs. [50–52] to enhance vessels. By modeling vessel appearance as ridge structures, the “vesselness,” or Frangi filter in Ref. [53] has been widely utilized to accent vessels over the rest of the image.

Combination of multiple images has also been based on the information redundancy that is provided when imaging the same tissue multiple times, using averaging [54], or blind deconvolution [55]. The central step in these approaches is image registration (see Section 4.2).

3.2 Tomographic imaging

In OCT imaging, noise reduction addresses an additional source of noise, besides conventional noise due to electronics. "Speckle noise" is an OCT artifact [56], due to the reflective nature of the retina. So-called "speckles" are due to the interference of the illumination with back-scattered light.

Generic, single-image noise reduction has been based on linear filtering [57], adaptive transforms [58], wavelets [59–63], and wave atom transformations [64]. Nonlinear filtering has also been proposed, using conventional [65] or multiscale anisotropic diffusion [66]. Other approaches include regularization [67], PCA [68], Bayesian inference [69], and stochastic methods [70]. Compressive sensing and sparse representations were proposed in Refs. [71–73]. A comparative evaluation of such approaches can be found in Ref. [74].

Nevertheless, the main focus of noise reduction approaches is on speckle noise reduction, as speckles significantly obscure retinal structure in the acquired images. The majority of noise reduction approaches averages multiple, uncorrelated scans of the same section. In this way, image structure due to transient speckle noise is attenuated over structure due to actual tissue. Some techniques include adaptations upon the conventional OCT apparatus, leading to more complex image acquisition. In these cases, acquisition of uncorrelated scans is based on modulation of the incidence angle of illumination [75–77], detection angle of back-scattered light [77], laser illumination frequency [78–80], and illumination polarization [81–83]. On the other hand, spatial compounding techniques [32–34, 84] do not require modification of the OCT scanner, as they use the purposeful motion of the scanner to acquire overlapping and adjacent scans. Motion is a priori known minus the uncertainty of mechanical motion and, thus, only minor alignment is required. As the aforementioned techniques image the same tissue multiple times, they are limited by eye motion (i.e., saccadic). Thereby, the brevity of acquisition time is required to reduce the probability of corresponding motion artifacts.

Accidental and purposeful motions call for scan alignment, through image registration (see Section 4.2). Once scans are registered, postprocessing further enhances the volumetric signal. In Refs. [32, 85], 3D wavelet filters are applied to volumetrically registered scans. In Ref. [86], volumetric neighborhoods are matched and averaged. In Ref. [87], a physical model of speckle formation is employed and estimated as a convex optimization problem upon the volumetric data.

4 Retinal image registration

The problem of image registration regards a test and a reference image. The goal is the estimation of the aligning transformation that warps the test image, so that retinal points in the warped image occur at the same pixel locations as in the reference image. RIR is challenging due to optical differences across modalities or devices, optical distortions due to the eye lens and vitreous humor, anatomical changes due to lesions or disease, as well as acquisition artifacts. Viewpoint differences (i.e., due to eye motion) complicate image registration further, due to projective distortion of the curved surface of the eye.

Applications of RIR can be classified according to whether images are acquired in the same or different examinations. Images from the same examination are devoid of anatomic changes. If their overlap is significant, they can be combined into images of higher resolution and definition [88–90], enabling more accurate measurements. Images with small overlap are utilized to create image mosaics that broaden the sensor's field of view [91–93] (see Fig. 1).

Longitudinal studies of the retina [97, 98] are facilitated by the registration of images acquired at different examinations (i.e., initial and follow-up). Pertinent studies enable disease monitoring and treatment evaluation, through tracking of symptom reversal. In this context, accurate registration of images of the same retinal region proves valuable in the detection of minute but critical changes, such as local hemorrhages or differences in vasculature width (see Fig. 2).

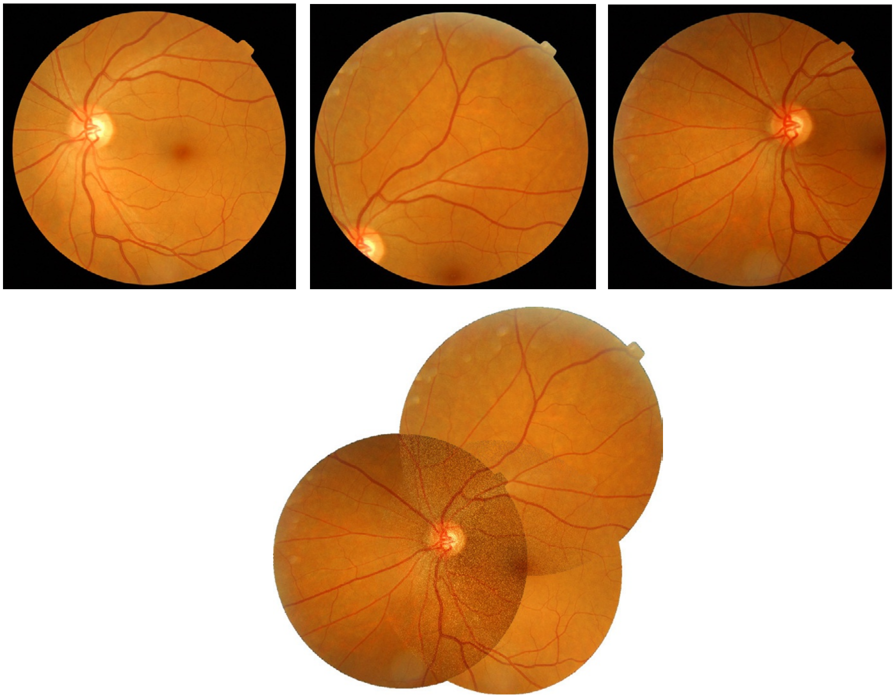

FIG. 1

Registration of retinal images into a mosaic. *Top*: Original images, from the public dataset in Refs. [94, 95]. *Bottom*: Registration result, using Hernandez-Matas [96].

From C. Hernandez-Matas, Retinal Image Registration Through 3D Eye Modelling and Pose Estimation (Ph.D. thesis), University of Crete, 2017.

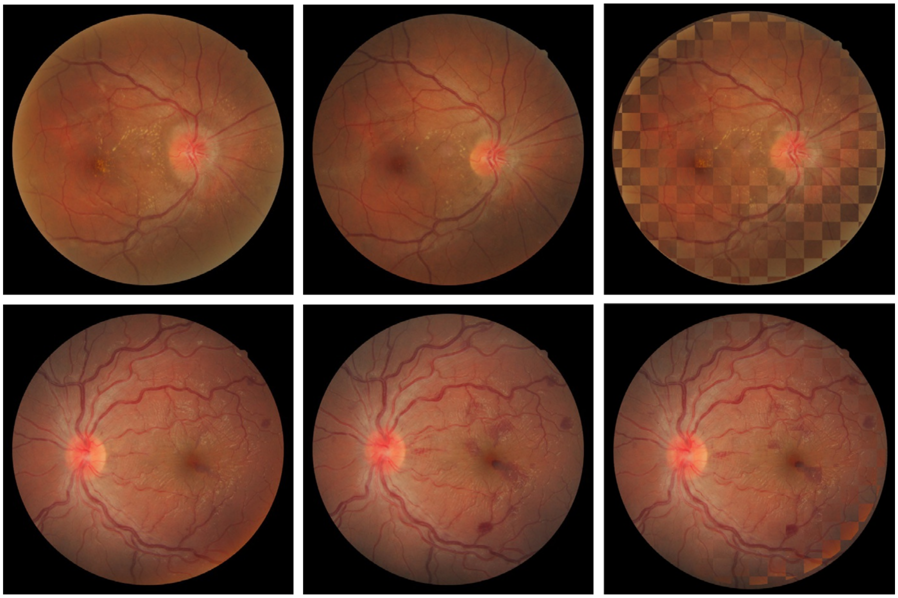

FIG. 2

Registration of fundus images from the same retinal region that exhibit differences, for longitudinal studies. *Left*: Original images from the public dataset in Refs. [99, 100]. *Right*: Registration results using Hernandez-Matas [96].

From C. Hernandez-Matas, Retinal Image Registration Through 3D Eye Modelling and Pose Estimation (Ph.D. thesis), University of Crete, 2017.

4.1 Fundus imaging

Initial approaches to RIR attempted similarity matching of the entire test and reference image as encoded in the spatial [101–106] or frequency [107] domains. A central assumption in global methods is that intensities in the test and reference image are consistent. However, this does not always hold due to uneven illumination, eye curvature, and anatomical changes that may occur between the acquisition of the test and reference images.

Instead of matching all image pixels, local approaches rely on matching well-localized features or keypoints [90, 92, 98, 103, 108–131] (see Fig. 3). The approaches in Refs. [117, 123] match feature points, based only on their topology. General purpose features associated with local descriptors have been more widely utilized for RIR. SIFT [132] features are the ones that have provided the greatest accuracy [109, 130], with SURF [133] features comprising a close second [126, 128]. Harris corners associated with a descriptor of their neighborhood have also been proposed [120, 126]. Features tuned to retinal structures include vessels, bifurcations, and crossovers [92, 114, 115]. As these features are not associated with descriptors, SIFT or SURF descriptors have been computed at their locations to

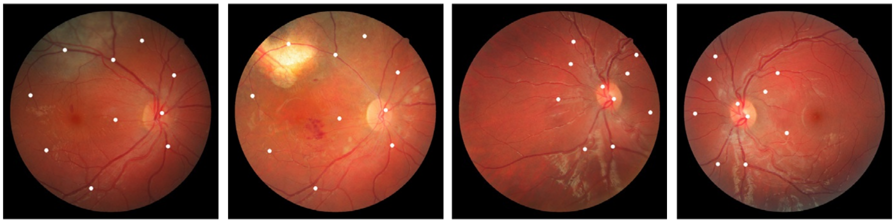

FIG. 3

Corresponding features in two pairs of retinal images, from the public dataset in Ref. [99, 100]. *White dots* show matched features.

From C. Hernandez-Matas, Retinal Image Registration Through 3D Eye Modelling and Pose Estimation (Ph.D. thesis), University of Crete, 2017.

facilitate matching [134]. In general, local methods have been more widely utilized, particularly for images with small overlap, due to the increased specificity that point matches provide. Moreover, local methods are more suitable for the registration of images with anatomical changes, as they are robust to partial image differences. In addition, they require less processing power, leading to faster registration.

At the heart of local approaches is the establishment of point correspondences, or matches, across the test and reference images. Pertinent methods utilize these correspondences to estimate a transform that, optimally, brings the matched points into coincidence. As some correspondences are spurious, robust estimation of the transform is utilized to relieve the result from their influence [90].

A range of 2D and 3D transforms has been utilized. Similarity transforms include rotation, scaling, translation, and modulation of aspect ratio [102–107, 110, 113, 114, 117, 119, 120, 124, 126, 127], while the affine transform is utilized to approximate projective distortion [92, 98, 101, 104, 110, 112–117, 117–120, 123–127, 131]. Projective transformations treat more appropriately perspective distortion at the cost of more degrees of freedom that imply higher computational cost and potential instability in optimization [90, 109, 110, 112, 128–130]. Quadratic transformations [92, 92, 104, 110, 111, 113, 114, 117, 119–122, 125, 125–127] allow further compensation for eye curvature. However, these transformations do not necessarily include consideration of the shape of the eye. Conversely, utilizing an eye model safeguards for unreasonable parameter model estimates and provides more accurate registration. In Refs. [96, 128–130], the RIR problem is formulated as a 3D pose estimation problem, solved by estimating the rigid transformation that relates the views from which the two images were acquired. Considering the problem in 3D enables 3D measurements, devoid of perspective distortion. Though 3D models account for perspective, they require knowledge of the shape of the imaged surface, either via modeling or via reconstruction. Even simple eye shape models have shown to improve registration accuracy of retinal images [128].

4.2 Tomographic imaging

Approaches to the registration of OCT images differ to fundus image registration approaches, due to their tomographic content. In some cases, OCT image registration is guided by the use of an additional fundus as a reference, which does not contain motion artifacts as it is instantaneously acquired.

Noise reduction in OCT images is based on averaging registered scans. In Ref. [32], the known translational motion of the scanner is assumed as accurate enough to juxtapose individual scans as volumetric data. In Ref. [33], an initial manual registration is refined through cross-correlation alignment. In Ref. [85], detecting the retinal pigment epithelium and requiring its continuity in adjacent scans provide a cue to registration. The work in Ref. [34] utilizes correlation maps of adjacent images. In Ref. [135], hierarchical affine-motion estimation approach is proposed. Low-rank and sparse image decomposition alignment has been employed in Ref. [136].

Eye motion estimation through OCT image registration has also been used to compensate for eye motion. In Ref. [137], an SLO-based eye tracker measured eye motion during image acquisition and images were registered according to these motion estimates. In Ref. [138], individual scans are registered to an SLO image. In Ref. [139], scans are registered without the use of a reference image; a particle filtering optimization is utilized to align scans in 3D as a dynamic system, which is optimized when adjacent scans are in consensus. In Ref. [140], registration is also optimization-based, but further exploits the temporal ordering of the scans and external information on their spatial arrangement. In Ref. [141], a semiautomatic approach is proposed to register and compare OCT scans, in order to study retinal changes in the corresponding data.

Mosaics of OCT volumes have been formed, using a fundus image as a reference. In Ref. [142], volumes are registered using vessel ridges and cross-correlation as a registration cue and based on the Iterative Closest Point algorithm. In Ref. [143], a reference image is not required, but adjacent volumes are registered based on a B-spline free-deformation method. In Ref. [144], a six-degree-of-freedom registration scheme for OCT volumes is proposed, which includes bundle adjustment corrections. In Refs. [145, 146], OCT volumes are registered in 3D without any prior knowledge of sensor or eye motion, based on correspondence of feature points.

4.3 Intramodal vs. cross-modal image registration

The combination of imaging modalities results in improved understanding of the retinal tissue and its pathologies. Cross-modal registration enables analysis and comparison of images that may emphasize complementary retinal features. In tomographic imaging, registration of axial scans to a frontal, fundus image enables registration of OCT scans, despite eye motion (see Section 4.2).

Methods in Refs. [112, 115, 116, 131] register fundus images and fluoroangiographies, by performing vessel segmentation and matching common vessel structures across the two cross-modal images. Vessel segmentation, detection, and matching of bifurcation points have been utilized to establish point correspondences across cross-modal images [113, 121]. Keypoint features, such as SIFT and SURF, and their descriptors have also been employed for the same purpose [92, 109, 114, 116, 117, 119, 120]. In addition, novel descriptors associated with conventional keypoints have been proposed [125, 125, 131].

In Refs. [101, 102], mutual information was proposed as a cue to the registration of fundus and SLO images. The methods in Refs. [138, 142] register frontal OCT scans with SLO images, in a similar fashion. As frontal images are visually similar across modalities, registration is achieved by conventional matching of vessels or vessel features.

More challenging is the registration of axial OCT scans with frontal fundus images. This registration facilitates the acquisition of a volumetric reconstruction of retinal tissue, below the retinal surface. The works in Refs. [147–149] utilize retinal vessels as the cue to the registration of frontal fundus images and axial OCT scans, requiring vessel segmentation as an initial step. However, as retinal vessel segmentation is still an open problem, vessel segmentation errors are propagated in the registration phase. In Ref. [150], a feature-based approach is proposed, which capitalizes on corner features as control points and utilizes histograms of oriented gradients to better match the neighborhoods of these points. A robust approach is also included to remove correspondence outliers and estimate the transform that better registers the OCT scans to the fundus image.

5 Conclusions

A wide range of methods exists for the preprocessing, enhancement, and registration of retinal images acquired by conventional and emerging imaging modalities.

The preprocessing and enhancement tasks are required in a broad variety of uses. The most straightforward is the inspection of the image by the medical professional, where preprocessing and enhancement are required to preserve the fidelity of the acquired image while clarifying or accenting its structure and anatomical features. Preprocessing and enhancement are also utilized as initial steps in algorithmic image analysis, to facilitate and increase the accuracy of detection, recognition, and measurement of anatomical features. For these cases, generic image preprocessing methods have been applied, though more recently, approaches carefully select and tailor image preprocessing according to the subsequent image analysis goals. Due to the aforementioned variety of uses, benchmarking of image preprocessing tasks has been difficult and scarce. In addition, as preprocessing is typically only part of an image analysis method, when evaluation is available it regards the entire method and not the image preprocessing part in isolation.

RIR is also the basis for a wide spectrum of tasks. First, registration of multiple images allows to combine them into improved or wider retinal images. Moreover, RIR has been employed the comparison of retinal images, which is essential for monitoring a disease and the assessment of its treatment. As image registration is a well-defined task, attempts to provide pertinent benchmarks are starting to appear, as in Ref. [99] where existing datasets for RIR are compared and a benchmark methodology is also proposed. Still, there is a clear need for new approaches to benchmarking that will allow for more direct comparisons of methods and will account for optical phenomena, such as optical distortions due to the eye lens, vitreous humor, and chromatic aberrations.

Acknowledgment

The authors thank Polykarpos Karamaounas for technical assistance in the preparation of the manuscript.

References

[1] M. Matsui, T. Tashiro, K. Matsumoto, S. Yamamoto, A study on automatic and quantitative diagnosis of fundus photographs (Transl. from Japanese), Nippon Ganka Gakkai Zasshi 77 (8) (1973) 907–918.
[2] A. Grosso, F. Veglio, M. Porta, F.M. Grignolo, T.Y. Wong, Hypertensive retinopathy revisited: some answers, more questions, Br. J. Ophthalmol. 89 (12) (2005) 1646–1654, https://doi.org/10.1136/bjo.2005.072546.
[3] R.P. Danis, M.D. Davis, Proliferative diabetic retinopathy, Diabetic Retinopathy, Humana Press, Totowa, NJ, 2008, pp. 29–65.
[4] A. Chernomorets, A. Krylov, Blur detection in fundus images, International Conference on BioMedical Engineering and Informatics, 2012, pp. 243–246.
[5] S. Mohammad, D. Morris, N. Thacker, Segmentation of optic disc in retina images using texture, International Conference on Computer Vision Theory and Applications, 2014, pp. 293–300.
[6] A. Fleming, S. Philip, K. Goatman, J. Olson, P. Sharp, Automated microaneurysm detection using local contrast normalization and local vessel detection, IEEE Trans. Med. Imaging 25 (9) (2006) 1223–1232.
[7] T. Walter, P. Massin, A. Erginay, R. Ordonez, C. Jeulin, J. Klein, Automatic detection of microaneurysms in color fundus images, Med. Image Anal. 11 (6) (2007) 555–566.
[8] A. Pujitha, G. Jahnavi, J. Sivaswamy, Detection of neovascularization in retinal images using semi-supervised learning, IEEE International Symposium on Biomedical Imaging, 2017, pp. 688–691.
[9] A. Deshmukh, T. Patil, S. Patankar, J. Kulkarni, Features based classification of hard exudates in retinal images, International Conference on Advances in Computing, Communications and Informatics, 2015, pp. 1652–1655.
[10] N. Salem, A. Nandi, Novel and adaptive contribution of the red channel in pre-processing of colour fundus images, J. Frankl. Inst. 344 (3) (2007) 243–256.
[11] C. Liu, M. Chang, Y. Chaung, S. Yu, A novel retinal image color texture enhancement method based on multi-regression analysis, International Symposium on Computer, Consumer and Control, 2016, pp. 793–796.
[12] J. Zhang, B. Dashtbozorg, E. Bekkers, J. Pluim, R. Duits, B.M. ter Haar Romeny, Robust

retinal vessel segmentation via locally adaptive derivative frames in orientation scores, IEEE Trans. Med. Imaging 35 (12) (2016) 2631–2644.
[13] J. Sivaswamy, A. Agarwal, M. Chawla, A. Rani, T. Das, Extraction of capillary non-perfusion from fundus fluorescein angiogram, A. Fred, J. Filipe, H. Gamboa (Eds.), Biomedical Engineering Systems and Technologies, Springer, Berlin, Heidelberg, 2009, pp. 176–188.
[14] Y. Zhao, Y. Liu, X. Wu, S. Harding, Y. Zheng, Retinal vessel segmentation: an efficient graph cut approach with Retinex and local phase, PLoS ONE 10 (4) (2015) 1–22.
[15] K. Zuiderveld, Contrast limited adaptive histogram equalization, Graphics Gems IV, Academic Press, San Diego, CA, 1994, pp. 474–485.
[16] G. Manikis, V. Sakkalis, X. Zabulis, P. Karamaounas, A. Triantafyllou, S. Douma, C. Zamboulis, K. Marias, An image analysis framework for the early assessment of hypertensive retinopathy signs, IEEE E-Health and Bioengineering Conference, 2011, pp. 1–6.
[17] U. Acharya, E. Ng, J. Tan, V. Sree, K. Ng, An integrated index for the identification of diabetic retinopathy stages using texture parameters, J. Med. Syst. 36 (3) (2012) 2011–2020.
[18] M. Zhou, K. Jin, S. Wang, J. Ye, D. Qian, Color retinal image enhancement based on luminosity and contrast adjustment, IEEE Trans. Biomed. Eng. 65 (3) (2018) 521–527.
[19] Sonali, S. Sahu, A. Singh, S. Ghrera, M. Elhoseny, An approach for de-noising and contrast enhancement of retinal fundus image using CLAHE, Opt. Laser Technol. 110 (2019) 87–98.
[20] A. Ajaz, B. Aliahmad, D. Kumar, A novel method for segmentation of infrared scanning laser ophthalmoscope (IR-SLO) images of retina, IEEE Engineering in Medicine and Biology Society, 2017, pp. 356–359.
[21] M. Esmaeili, H. Rabbani, A.M. Dehnavi, Automatic optic disk boundary extraction by the use of curvelet transform and deformable variational level set model, Pattern Recogn. 45 (7) (2012) 2832–2842, https://doi.org/10.1016/j.patcog.2012.01.002.
[22] A. Sopharak, B. Uyyanonvara, S. Barman, T. Williamson, Automatic detection of diabetic retinopathy exudates from non-dilated retinal images using mathematical morphology methods, Comput. Med. Imaging Graph. 32 (2008) 720–727.
[23] S.M. Shankaranarayana, K. Ram, A. Vinekar, K. Mitra, M. Sivaprakasam, Restoration of neonatal retinal images, Proceedings of the Ophthalmic Medical Image Analysis Third International Workshop, OMIA, 2016, pp. 49–56.
[24] A. Aibinu, M. Iqbal, M. Nilsson, M. Salami, A new method of correcting uneven illumination problem in fundus images, International Conference on Robotics, Vision, Information, and Signal Processing, 2007, pp. 445–449.
[25] K. Huang, M. Yan, A local adaptive algorithm for microaneurysms detection in digital fundus images, Computer Vision for Biomedical Image Applications, 2005, pp. 103–113.
[26] R. GeethaRamani, L. Balasubramanian, Retinal blood vessel segmentation employing image processing and data mining techniques for computerized retinal image analysis. Retinal blood vessel segmentation in fundus images, Biocybern. Biomed. Eng. 36 (1) (2016) 102–118.
[27] M. Foracchia, E. Grisan, A. Ruggeri, Luminosity and contrast normalization in retinal images, Med. Image Anal. 9 (3) (2005) 179–190.
[28] H. Narasimha-Iyer, A. Can, B. Roysam, V. Stewart, H.L. Tanenbaum, A. Majerovics, H. Singh, Robust detection and classification of longitudinal changes in color retinal

fundus images for monitoring diabetic retinopathy, IEEE Trans. Biomed. Eng. 53 (6) (2006) 1084–1098.
[29] E. Grisan, A. Giani, E. Ceseracciu, A. Ruggeri, Model-based illumination correction in retinal images, IEEE International Symposium on Biomedical Imaging: Nano to Macro, 2006, pp. 984–987.
[30] R. Kolar, J. Odstrcilik, J. Jan, V. Harabis, Illumination correction and contrast equalization in colour fundus images, European Signal Processing Conference, 2011, pp. 298–302.
[31] A. Lang, A. Carass, M. Hauser, E. Sotirchos, P. Calabresi, H. Ying, J. Prince, Retinal layer segmentation of macular OCT images using boundary classification, Biomed. Opt. Express 4 (7) (2013) 1133–1152.
[32] M. Avanaki, R. Cernat, P. Tadrous, T. Tatla, A. Podoleanu, S. Hojjatoleslami, Spatial compounding algorithm for speckle reduction of dynamic focus OCT images, IEEE Photon. Technol. Lett. 25 (2013) 1439–1442.
[33] M. Mayer, A. Borsdorf, M. Wagner, J. Hornegger, C. Mardin, R. Tornow, Wavelet denoising of multiframe optical coherence tomography data, Biomed. Opt. Express 3 (3) (2012) 572–589.
[34] M. Jorgensen, J. Thomadsen, U. Christensen, W. Soliman, B. Sander, Enhancing the signal-to-noise ratio in ophthalmic optical coherence tomography by image registration method and clinical examples, J. Biomed. Opt. 12 (4) (2007) 041208.
[35] R. Phillips, J. Forrester, P. Sharp, Automated detection and quantification of retinal exudates, Graefe's Arch. Clin. Exp. Ophthalmol. 231 (2) (1993) 90–94.
[36] N. Patton, T. Aslam, T. MacGillivray, I. Deary, B. Dhillon, R. Eikelboom, K. Yogesan, I. Constable, Retinal image analysis: concepts, applications and potential, Prog. Retin. Eye Res. 25 (1) (2006) 99–127.
[37] E. Peli, T. Peli, Restoration of retinal images obtained through cataracts, IEEE Trans. Med. Imaging 8 (4) (1989) 401–406.
[38] U. Qidwai, U. Qidwai, Blind deconvolution for retinal image enhancement, IEEE EMBS Conference on Biomedical Engineering and Sciences, 2010, pp. 20–25.
[39] P. Dai, H. Sheng, J. Zhang, L. Li, J. Wu, M. Fan, Retinal fundus image enhancement using the normalized convolution and noise removing, J. Biomed. Imaging 2016 (2016) 1–12.
[40] J. Soares, J. Leandro, R. Cesar, H. Jelinek, M. Cree, Retinal vessel segmentation using the 2-D Gabor wavelet and supervised classification, IEEE Trans. Med. Imaging 25 (9) (2006) 1214–1222.
[41] T.R. Mengko, A. Handayani, V.V. Valindria, S. Hadi, I. Sovani, Image processing in retinal angiography: extracting angiographical features without the requirement of contrast agents, Proceedings of the IAPR Conference on Machine Vision Applications (IAPR MVA 2009), Keio University, Yokohama, Japan, May 20–22, 2009, pp. 451–454.
[42] P. Feng, Y. Pan, B. Wei, W. Jin, D. Mi, Enhancing retinal image by the Contourlet transform, Pattern Recogn. Lett. 28 (4) (2007) 516–522.
[43] X. Bai, F. Zhou, B. Xue, Image enhancement using multi scale image features extracted by top-hat transform, Opt. Laser Technol. 44 (2) (2012) 328–336.
[44] R. Kromer, R. Shafin, S. Boelefahr, M. Klemm, An automated approach for localizing retinal blood vessels in confocal scanning laser ophthalmoscopy fundus images, J. Med. Biol. Eng. 36 (4) (2016) 485–494.
[45] J. Xu, H. Ishikawa, G. Wollstein, J. Schuman, Retinal vessel segmentation on SLO image, IEEE Eng. Med. Biol. Soc. 2008 (2008) 2258–2261.
[46] H. Rampal, R. Kumar, B. Ramanathan, T. Das, Complex shock filtering applied to retinal

image enhancement, World Congress on Medical Physics and Biomedical Engineering, 2013, pp. 900–903.
[47] L. Wang, G. Liu, S. Fu, L. Xu, K. Zhao, C. Zhang, Retinal image enhancement using robust inverse diffusion equation and self-similarity filtering, PLoS ONE 11 (7) (2016) 1–13.
[48] B. Chen, Y. Chen, Z. Shao, T. Tong, L. Luo, Blood vessel enhancement via multi-dictionary and sparse coding: Application to retinal vessel enhancing, Neurocomputing 200 (2016) 110–117.
[49] A. Marrugo, M. Millán, M. Sorel, J. Kotera, F. Sroubek, Improving the blind restoration of retinal images by means of point-spread-function estimation assessment, International Symposium on Medical Information Processing and Analysis, vol. 9287, 2015, p. 92871D.
[50] A. Hoover, V. Kouznetsova, M. Goldbaum, Locating blood vessels in retinal images by piecewise threshold probing of a matched filter response, IEEE Trans. Med. Imaging 19 (3) (2000) 203–210.
[51] T. Lin, M. Du, J. Xu, The preprocessing of subtraction and the enhancement for biomedical image of retinal blood vessels, J. Biomed. Eng. 1 (20) (2003) 56–59.
[52] S. Chaudhuri, S. Chatterjee, N. Katz, M. Nelson, M. Goldbaum, Detection of blood vessels in retinal images using two-dimensional matched filters, IEEE Trans. Med. Imaging 8 (3) (1989) 263–269.
[53] A.F. Frangi, W.J. Niessen, K.L. Vincken, M.A. Viergever, Multiscale vessel enhancement filtering, Medical Image Computing and Computer-Assisted Intervention—MICCAI'98: First International Conference Cambridge, MA, USA, October 11–13, 1998 Proceedings, Springer, Berlin, Heidelberg, 1998, pp. 130–137, https://doi.org/10.1007/BFb0056195.
[54] S. Crespo-Garcia, N. Reichhart, C. Hernandez-Matas, X. Zabulis, N. Kociok, C. Brockmann, A. Joussen, O. Strauss, In-vivo analysis of the time and spatial activation pattern of microglia in the retina following laser-induced choroidal neovascularization, Exp. Eye Res. 139 (2015) 13–21.
[55] A. Marrugo, M. Millan, M. Sorel, F. Sroubek, Retinal image restoration by means of blind deconvolution, J. Biomed. Opt. 16 (11) (2011) 1–16.
[56] J. Schmitt, A. Knüttel, Model of optical coherence tomography of heterogeneous tissue, J. Opt. Soc. Am. A 14 (6) (1997) 1231–1242.
[57] M. Pircher, E. Götzinger, R. Leitgeb, A. Fercher, C. Hitzenberger, Measurement and imaging of water concentration in human cornea with differential absorption optical coherence tomography, Opt. Express 11 (18) (2003) 2190–2197.
[58] J. Rogowska, M. Brezinski, Evaluation of the adaptive speckle suppression filter for coronary optical coherence tomography imaging, IEEE Trans. Med. Imaging 19 (12) (2000) 1261–1266.
[59] Z. Jian, Z. Yu, L. Yu, B. Rao, Z. Chen, B. Tromberg, Speckle attenuation in optical coherence tomography by curvelet shrinkage, Opt. Lett. 34 (10) (2009) 1516–1518.
[60] S. Chitchian, M.A. Mayer, A.R. Boretsky, F.J. van Kuijk, M. Motamedi, Retinal optical coherence tomography image enhancement via shrinkage denoising using double-density dual-tree complex wavelet transform, J. Biomed. Opt. 17 (11) (2012) 116009.
[61] Q. Guo, F. Dong, S. Sun, B. Lei, B. Gao, Image denoising algorithm based on contourlet transform for optical coherence tomography heart tube image, IET Image Process. 7 (5) (2013) 442–450.
[62] D.C. Adler, T.H. Ko, J.G. Fujimoto, Speckle reduction in optical coherence tomography images by use of a spatially adaptive wavelet filter, Opt. Lett. 29 (24) (2004) 2878–

2880, https://doi.org/10.1364/OL.29.002878.
[63] P. Puvanathasan, K. Bizheva, Speckle noise reduction algorithm for optical coherence tomography based on interval type II fuzzy set. Opt. Express 15 (24) (2007) 15747–15758, https://doi.org/10.1364/OE.15.015747.
[64] Y. Du, G. Liu, G. Feng, Z. Chen, Speckle reduction in optical coherence tomography images based on wave atoms, J. Biomed. Opt. 19 (5) (2014) 1–7.
[65] H. Salinas, D. Fernandez, Comparison of PDE-based nonlinear diffusion approaches for image enhancement and denoising in optical coherence tomography, IEEE Trans. Med. Imaging 26 (6) (2007) 761–771.
[66] F. Zhang, Y. Yoo, L. Koh, Y. Kim, Nonlinear diffusion in Laplacian pyramid domain for ultrasonic speckle reduction, IEEE Trans. Med. Imaging 26 (2007) 200–211.
[67] D. Marks, T. Ralston, S. Boppart, Speckle reduction by I-divergence regularization in optical coherence tomography, J. Opt. Soc. Am. 22 (11) (2005) 2366–2371.
[68] H. Lv, S. Fu, C. Zhang, L. Zhai, Speckle noise reduction of multi-frame optical coherence tomography data using multi-linear principal component analysis, Opt. Express 26 (9) (2018) 11804–11818.
[69] A. Wong, A. Mishra, K. Bizheva, D. Clausi, General Bayesian estimation for speckle noise reduction in optical coherence tomography retinal imagery, Opt. Express 18 (8) (2010) 8338–8352.
[70] A. Cameron, D. Lui, A. Boroomand, J. Glaister, A. Wong, K. Bizheva, Stochastic speckle noise compensation in optical coherence tomography using non-stationary spline-based speckle noise modelling, Biomed. Opt. Express 4 (9) (2013) 1769–1785.
[71] L. Fang, S. Li, Q. Nie, J. Izatt, C. Toth, S. Farsiu, Sparsity based denoising of spectral domain optical coherence tomography images, Biomed. Opt. Express 3 (5) (2012) 927–942.
[72] L. Fang, S. Li, R. McNabb, Q. Nie, A. Kuo, C. Toth, J. Izatt, S. Farsiu, Fast acquisition and reconstruction of optical coherence tomography images via sparse representation, IEEE Trans. Med. Imaging 32 (2013) 2034–2049.
[73] D. Thapa, K. Raahemifar, V. Lakshminarayanan, A new efficient dictionary and its implementation on retinal images, International Conference on Digital Signal Processing, 2014, pp. 841–846.
[74] A. Ozcan, A. Bilenca, A. Desjardins, B. Bouma, G. Tearney, Speckle reduction in optical coherence tomography images using digital filtering, J. Opt. Soc. Am. 24 (7) (2007) 1901–1910.
[75] N. Iftimia, B. Bouma, G. Tearney, Speckle reduction in optical coherence tomography by “path length encoded” angular compounding, J. Biomed. Opt. 8 (2003) 260–263.
[76] H. Wang, A.M. Rollins, OCT speckle reduction with angular compounding by B-scan Doppler-shift encoding, Proc. SPIE, 7168, 2009, https://doi.org/10.1117/12.809852.
[77] A. Desjardins, B. Vakoc, W. Oh, S. Motaghiannezam, G. Tearney, B. Bouma, Angle-resolved optical coherence tomography with sequential angular selectivity for speckle reduction, Opt. Express 15 (10) (2007) 6200–6209.
[78] M. Pircher, E. Götzinger, R. Leitgeb, A. Fercher, C. Hitzenberger, Speckle reduction in optical coherence tomography by frequency compounding, J. Biomed. Opt. 8 (3) (2003) 565–569.
[79] J. Kim, D.T. Miller, E.K. Kim, S. Oh, J.H. Oh, T.E. Milner, Optical coherence tomography speckle reduction by a partially spatially coherent source, J. Biomed. Opt. 10 (2005) 064034, https://doi.org/10.1117/1.2138031.
[80] B. Karamata, P. Lambelet, M. Laubscher, R.P. Salathé, T. Lasser, Spatially incoherent illumination as a mechanism for cross-talk suppression in wide-field optical coherence

tomography, Opt. Lett. 29 (7) (2004) 736–738, https://doi.org/10.1364/OL.29.000736.
[81] H. Ren, Z. Ding, Y. Zhao, J. Miao, J.S. Nelson, Z. Chen, Phase-resolved functional optical coherence tomography: simultaneous imaging of in situ tissue structure, blood flow velocity, standard deviation, birefringence, and Stokes vectors in human skin, Opt. Lett. 27 (19) (2002) 1702–1704, https://doi.org/10.1364/OL.27.001702.
[82] M. Kobayashi, H. Hanafusa, K. Takada, J. Noda, Polarization-independent interferometric optical-time-domain reflectometer, J. Lightwave Technol. 9 (5) (1991) 623–628.
[83] J. Schmitt, Array detection for speckle reduction in optical coherence microscopy, Phys. Med. Biol. 42 (7) (1997) 1427.
[84] R.J. Zawadzki, B. Cense, Y. Zhang, S.S. Choi, D.T. Miller, J.S. Werner, Ultrahigh-resolution optical coherence tomography with monochromatic and chromatic aberration correction, Opt. Express 16 (11) (2008) 8126–8143, https://doi.org/10.1364/OE.16.008126.
[85] Z. Jian, L. Yu, B. Rao, B. Tromberg, Z. Chen, Three-dimensional speckle suppression in optical coherence tomography based on the curvelet transform, Opt. Express 18 (2) (2010) 1024–1032.
[86] C. Gyger, R. Cattin, P. Hasler, P. Maloca, Three-dimensional speckle reduction in optical coherence tomography through structural guided filtering, Opt. Eng. 53 (7) (2014) 1024–1032.
[87] L. Bian, J. Suo, F. Chen, Q. Dai, Multiframe denoising of high-speed optical coherence tomography data using interframe and intraframe priors, J. Biomed. Opt. 20 (2015) 36006.
[88] N. Meitav, E.N. Ribak, Improving retinal image resolution with iterative weighted shift-and-add, J. Opt. Soc. Am. A 28 (7) (2011) 1395–1402, https://doi.org/10.1364/JOSAA.28.001395.
[89] G. Molodij, E.N. Ribak, M. Glanc, G. Chenegros, Enhancing retinal images by extracting structural information, Opt. Commun. 313 (2014) 321–328, https://doi.org/10.1016/j.optcom.2013.10.011.
[90] C. Hernandez-Matas, X. Zabulis, Super resolution for fundoscopy based on 3D image registration, 36th Annual International Conference of the IEEE Engineering in Medicine and Biology Society, 2014, pp. 6332–6338, https://doi.org/10.1109/EMBC.2014.6945077.
[91] A. Can, C.V. Stewart, B. Roysam, H.L. Tanenbaum, A feature-based technique for joint, linear estimation of high-order image-to-mosaic transformations: mosaicing the curved human retina, IEEE Trans. Pattern Anal. Mach. Intell. 24 (3) (2002) 412–419, https://doi.org/10.1109/34.990145.
[92] N. Ryan, C. Heneghan, P. de Chazal, Registration of digital retinal images using landmark correspondence by expectation maximization, Image Vis. Comput. 22 (11) (2004) 883–898, https://doi.org/10.1016/j.imavis.2004.04.004.
[93] P.C. Cattin, H. Bay, L. Van Gool, G. Székely, Retina mosaicing using local features, Medical Image Computing and Computer-Assisted Intervention—MICCAI 2006: 9th International Conference, Copenhagen, Denmark, October 1–6, 2006. Proceedings, Part II, Springer, Berlin, Heidelberg, 2006, pp. 185–192.
[94] K.M. Adal, P.G. van Etten, J.P. Martinez, L.J. van Vliet, K.A. Vermeer, Accuracy assessment of intra- and intervisit fundus image registration for diabetic retinopathy screening. Invest. Ophthalmol. Vis. Sci. 56 (3) (2015) 1805–1812, https://doi.org/10.1167/iovs.14-15949.

[95] RODREP: Rotterdam ophthalmic data repository longitudinal diabetic retinopathy screening data, Available from: http://www.rodrep.com/longitudinal-diabetic-retinopathy-screening--description.html (Accessed 25 May 2017).
[96] C. Hernandez-Matas, Retinal Image Registration Through 3D Eye Modelling and Pose Estimation (Ph.D. thesis), University of Crete, 2017.
[97] H. Narasimha-Iyer, A. Can, B. Roysam, H.L. Tanenbaum, A. Majerovics, Integrated analysis of vascular and nonvascular changes from color retinal fundus image sequences, IEEE Trans. Biomed. Eng. 54 (8) (2007) 1436–1445, https://doi.org/10.1109/TBME.2007.900807.
[98] G. Troglio, J.A. Benediktsson, G. Moser, S.B. Serpico, E. Stefansson, Unsupervised change detection in multitemporal images of the human retina, Multi Modality State-of-the-Art Medical Image Segmentation and Registration Methodologies, vol. 1, Springer US, Boston, MA, 2011, pp. 309–337.
[99] C. Hernandez-Matas, X. Zabulis, A. Triantafyllou, P. Anyfanti, S. Douma, A.A. Argyros, FIRE: fundus image registration dataset, J. Model. Ophthalmol. 1 (4) (2017) 16–28.
[100] FIRE: fundus image registration dataset, Available from: http://www.ics.forth.gr/cvrl/fire (Accessed 18 May 2019).
[101] P.S. Reel, L.S. Dooley, K.C.P. Wong, A. Börner, Robust retinal image registration using expectation maximisation with mutual information, IEEE International Conference on Acoustics, Speech and Signal Processing, 2013, pp. 1118–1122, https://doi.org/10.1109/ICASSP.2013.6637824.
[102] P.A. Legg, P.L. Rosin, D. Marshall, J.E. Morgan, Improving accuracy and efficiency of mutual information for multi-modal retinal image registration using adaptive probability density estimation, Comput. Med. Imaging Graph. 37 (7–8) (2013) 597–606, https://doi.org/10.1016/j.compmedimag.2013.08.004.
[103] E. Peli, R.A. Augliere, G.T. Timberlake, Feature-based registration of retinal images, IEEE Trans. Med. Imaging 6 (3) (1987) 272–278, https://doi.org/10.1109/TMI.1987.4307837.
[104] K.M. Adal, R.M. Ensing, R. Couvert, P. van Etten, J.P. Martinez, K.A. Vermeer, L.J. van Vliet, A hierarchical coarse-to-fine approach for fundus image registration, Biomedical Image Registration. WBIR 2014. Lecture Notes in Computer Science, 8545, 2014, pp. 93–102.
[105] J. Noack, D. Sutton, An algorithm for the fast registration of image sequences obtained with a scanning laser ophthalmoscope, Phys. Med. Biol. 39 (5) (1994) 907.
[106] A. Wade, F. Fitzke, A fast, robust pattern recognition system for low light level image registration and its application to retinal imaging, Opt. Express 3 (5) (1998) 190–197.
[107] A.V. Cideciyan, S.G. Jacobson, C.M. Kemp, R.W. Knighton, J.H. Nagel, Registration of high resolution images of the retina, SPIE Med. Imaging 1652 (1992) 310–322, https://doi.org/10.1117/12.59439.
[108] Z. Li, F. Huang, J. Zhang, B. Dashtbozorg, S. Abbasi-Sureshjani, Y. Sun, X. Long, Q. Yu, B. ter Haar Romeny, T. Tan, Multi-modal and multi-vendor retina image registration, Biomed. Opt. Express 9 (2) (2018) 410–422.
[109] Y. Lin, G. Medioni, Retinal image registration from 2D to 3D, IEEE Conference on Computer Vision and Pattern Recognition, 2008, pp. 1–8, https://doi.org/10.1109/CVPR.2008.4587705.
[110] J. Zheng, J. Tian, K. Deng, X. Dai, X. Zhang, M. Xu, Salient feature region: a new method for retinal image registration, IEEE Trans. Inf. Technol. Biomed. 15 (2) (2011) 221–232, https://doi.org/10.1109/TITB.2010.2091145.

[111] S.K. Saha, D. Xiao, S. Frost, Y. Kanagasingam, A two-step approach for longitudinal registration of retinal images, J. Med. Syst. 40 (12) (2016) 277, https://doi.org/10.1007/s10916-016-0640-0.
[112] G.K. Matsopoulos, N.A. Mouravliansky, K.K. Delibasis, K.S. Nikita, Automatic retinal image registration scheme using global optimization techniques, IEEE Trans. Inf. Technol. Biomed. 3 (1) (1999) 47–60, https://doi.org/10.1109/4233.748975.
[113] F. Laliberte, L. Gagnon, Y. Sheng, Registration and fusion of retinal images—an evaluation study, IEEE Trans. Med. Imaging 22 (5) (2003) 661–673, https://doi.org/10.1109/TMI.2003.812263.
[114] C.V. Stewart, C.-L. Tsai, B. Roysam, The dual-bootstrap iterative closest point algorithm with application to retinal image registration, IEEE Trans. Med. Imaging 22 (11) (2003) 1379–1394, https://doi.org/10.1109/TMI.2003.819276.
[115] G.K. Matsopoulos, P.A. Asvestas, N.A. Mouravliansky, K.K. Delibasis, Multimodal registration of retinal images using self organizing maps, IEEE Trans. Med. Imaging 23 (12) (2004) 1557–1563, https://doi.org/10.1109/TMI.2004.836547.
[116] T.E. Choe, G. Medioni, I. Cohen, A.C. Walsh, S.R. Sadda, 2-D registration and 3-D shape inference of the retinal fundus from fluorescein images. Med. Image Anal. 12 (2) (2008) 174–190, https://doi.org/10.1016/j.media.2007.10.002.
[117] G. Yang, C.V. Stewart, M. Sofka, C.L. Tsai, Registration of challenging image pairs: initialization, estimation, and decision, IEEE Trans. Pattern Anal. Mach. Intell. 29 (11) (2007) 1973–1989, https://doi.org/10.1109/TPAMI.2007.1116.
[118] A.R. Chaudhry, J.C. Klein, Ophthalmologic image registration based on shape-context: application to Fundus Autofluorescence (FAF) images, Visualization, Imaging, and Image Processing (VIIP), September, Palma de Mallorca, Spain. Medical Imaging, track 630-055, 2008.
[119] C.L. Tsai, C.Y. Li, G. Yang, K.S. Lin, The edge-driven dual-bootstrap iterative closest point algorithm for registration of multimodal fluorescein angiogram sequence, IEEE Trans. Med. Imaging 29 (3) (2010) 636–649, https://doi.org/10.1109/TMI.2009.2030324.
[120] J. Chen, J. Tian, N. Lee, J. Zheng, R.T. Smith, A.F. Laine, A partial intensity invariant feature descriptor for multimodal retinal image registration, IEEE Trans. Biomed. Eng. 57 (7) (2010) 1707–1718, https://doi.org/10.1109/TBME.2010.2042169.
[121] K. Deng, J. Tian, J. Zheng, X. Zhang, X. Dai, M. Xu, Retinal fundus image registration via vascular structure graph matching, J. Biomed. Imaging 2010 (2010) 14:1–14:13, https://doi.org/10.1155/2010/906067.
[122] A. Perez-Rovira, R. Cabido, E. Trucco, S.J. McKenna, J.P. Hubschman, RERBEE: robust efficient registration via bifurcations and elongated elements applied to retinal fluorescein angiogram sequences, IEEE Trans. Med. Imaging 31 (1) (2012) 140–150, https://doi.org/10.1109/TMI.2011.2167517.
[123] S. Gharabaghi, S. Daneshvar, M.H. Sedaaghi, Retinal image registration using geometrical features, J. Dig. Imaging 26 (2) (2013) 248–258, https://doi.org/10.1007/s10278-012-9501-7.
[124] L. Chen, X. Huang, J. Tian, Retinal image registration using topological vascular tree segmentation and bifurcation structures, Biomed. Signal Process. Control 16 (2015) 22–31, https://doi.org/10.1016/j.bspc.2014.10.009.
[125] J.A. Lee, J. Cheng, B.H. Lee, E.P. Ong, G. Xu, D.W.K. Wong, J. Liu, A. Laude, T.H. Lim, A low-dimensional step pattern analysis algorithm with application to multimodal retinal image registration, IEEE Conference on Computer Vision and Pattern Recognition (CVPR), 2015, pp. 1046–1053, https://doi.org/10.1109/CVPR.2015.7298707.
[126] G. Wang, Z. Wang, Y. Chen, W. Zhao, Robust point matching method for multimodal

retinal image registration, Biomed. Signal Process. Control 19 (2015) 68–76, https://doi.org/10.1016/j.bspc.2015.03.004.
[127] Z. Ghassabi, J. Shanbehzadeh, A. Mohammadzadeh, A structure-based region detector for high-resolution retinal fundus image registration, Biomed. Signal Process. Control 23 (2016) 52–61, https://doi.org/10.1016/j.bspc.2015.08.005.
[128] C. Hernandez-Matas, X. Zabulis, A.A. Argyros, Retinal image registration based on keypoint correspondences, spherical eye modeling and camera pose estimation, 37th Annual International Conference of the IEEE Engineering in Medicine and Biology Society (EMBC), 2015, pp. 5650–5654, https://doi.org/10.1109/EMBC.2015.7319674.
[129] C. Hernandez-Matas, X. Zabulis, A. Triantafyllou, P. Anyfanti, A.A. Argyros, Retinal image registration under the assumption of a spherical eye, Comput. Med. Imaging Graph. 55 (2017) 95–105, https://doi.org/10.1016/j.compmedimag.2016.06.006.
[130] C. Hernandez-Matas, X. Zabulis, A.A. Argyros, Retinal image registration through simultaneous camera pose and eye shape estimation, 38th Annual International Conference of the IEEE Engineering in Medicine and Biology Society (EMBC), 2016, pp. 3247–3251, https://doi.org/10.1109/EMBC.2016.7591421.
[131] C. Liu, J. Ma, Y. Ma, J. Huang, Retinal image registration via feature-guided Gaussian mixture model, J. Opt. Soc. Am. A 33 (7) (2016) 1267–1276, https://doi.org/10.1364/JOSAA.33.001267.
[132] D.G. Lowe, Distinctive image features from scale-invariant keypoints, Int. J. Comput. Vis. 60 (2) (2004) 91–110, https://doi.org/10.1023/B:VISI.0000029664.99615.94.
[133] H. Bay, A. Ess, T. Tuytelaars, L.V. Gool, Speeded-up robust features (SURF), Comput. Vis. Image Underst. 110 (3) (2008) 346–359, https://doi.org/10.1016/j.cviu.2007.09.014.
[134] C. Hernandez-Matas, X. Zabulis, A.A. Argyros, An experimental evaluation of the accuracy of keypoints-based retinal image registration, 39th Annual International Conference of the IEEE Engineering in Medicine and Biology Society (EMBC), 2017, pp. 377–381.
[135] D. Alonso-Caneiro, S. Read, M. Collins, Speckle reduction in optical coherence tomography imaging by affine-motion image registration, J. Biomed. Opt. 16 (11) (2011) 116027.
[136] A. Baghaie, R. D'Souza, Z. Yu, Sparse and low rank decomposition based batch image alignment for speckle reduction of retinal OCT images, International Symposium on Biomedical Imaging, 2015, pp. 226–230.
[137] M. Pircher, B. Baumann, E. Götzinger, H. Sattmann, C. Hitzenberger, Simultaneous SLO/OCT imaging of the human retina with axial eye motion correction, Opt. Express 15 (25) (2007) 16922–16932.
[138] S. Ricco, M. Chen, H. Ishikawa, G. Wollstein, J. Schuman, Correcting motion artifacts in retinal spectral domain optical coherence tomography via image registration, Med. Image Comput. Comput. Assist. Interv. 12 (1) (2009) 100–107.
[139] J. Xu, H. Ishikawa, G. Wollstein, L. Kagemann, J. Schuman, Alignment of 3-D optical coherence tomography scans to correct eye movement using a particle filtering, IEEE Trans. Med. Imaging 31 (2012) 1337–1345.
[140] M. Kraus, J. Liu, J. Schottenhamml, C. Chen, A. Budai, L. Branchini, T. Ko, H. Ishikawa, G. Wollstein, J. Schuman, J. Duker, J. Fujimoto, J. Hornegger, Quantitative 3D-OCT motion correction with tilt and illumination correction, robust similarity measure and regularization, Biomed. Opt. Express 5 (8) (2014) 2591–2613.
[141] M. Röhlig, C. Schmidt, R.K. Prakasam, P. Rosenthal, H. Schumann, O. Stachs, Visual

analysis of retinal changes with optical coherence tomography, Vis. Comput. 34 (9) (2018) 1209–1224, https://doi.org/10.1007/s00371-018-1486-x.
[142] Y. Li, G. Gregori, R. Knighton, B. Lujan, P. Rosenfeld, Registration of OCT fundus images with color fundus photographs based on blood vessel ridges, Opt. Express 19 (1) (2011) 7–16.
[143] H. Hendargo, R. Estrada, S. Chiu, C. Tomasi, S. Farsiu, J. Izatt, Automated non-rigid registration and mosaicing for robust imaging of distinct retinal capillary beds using speckle variance optical coherence tomography, Biomed. Opt. Express 4 (6) (2013) 803–821.
[144] K. Lurie, R. Angst, A. Ellerbee, Automated mosaicing of feature-poor optical coherence tomography volumes with an integrated white light imaging system, IEEE Trans. Biomed. Eng. 61 (7) (2014) 2141–2153.
[145] M. Niemeijer, M.K. Garvin, K. Lee, B. van Ginneken, M.D. Abràmoff, M. Sonka, Registration of 3D spectral OCT volumes using 3D SIFT feature point matching, Proc. SPIE, 7259, 2009, https://doi.org/10.1117/12.811906.
[146] M. Niemeijer, K. Lee, M.K. Garvin, M.D. Abràmoff, M. Sonka, Registration of 3D spectral OCT volumes combining ICP with a graph-based approach, Proc. SPIE, 8314, 2012, https://doi.org/10.1117/12.911104.
[147] M.S. Miri, M.D. Abramoff, K. Lee, M. Niemeijer, J. Wang, Y.H. Kwon, M.K. Garvin, Multimodal segmentation of optic disc and cup from SD-OCT and color fundus photographs using a machine-learning graph-based approach, IEEE Trans. Med. Imaging 34 (9) (2015) 1854–1866, https://doi.org/10.1109/TMI.2015.2412881.
[148] R. Kolar, P. Tasevsky, Registration of 3D retinal optical coherence tomography data and 2D fundus images, Biomedical Image Registration, 2010, pp. 72–82.
[149] M. Golabbakhsh, H. Rabbani, Vessel-based registration of fundus and optical coherence tomography projection images of retina using a quadratic registration model, IET Image Process. 7 (8) (2013) 768–776.
[150] M.S. Miri, M.D. Abràmoff, Y.H. Kwon, M.K. Garvin, Multimodal registration of SD-OCT volumes and fundus photographs using histograms of oriented gradients, Biomed. Opt. Express 7 (12) (2016) 5252–5267, https://doi.org/10.1364/BOE.7.005252.